Theoretical Study of the Crystal-Field Energy Levels and Two-Photon Absorption Intensities of Tb3+ in Cubic Host Lattices

ARTICLE *in* THE JOURNAL OF PHYSICAL CHEMISTRY A · FEBRUARY 2011

Impact Factor: 2.69 · DOI: 10.1021/jp111620e · Source: PubMed

2 AUTHORS:

Chang-Kui Duan
University of Science and Technology of China
177 PUBLICATIONS **1,811** CITATIONS
SEE PROFILE

Peter Anthony Tanner
The Hong Kong Institute of Education
355 PUBLICATIONS **4,367** CITATIONS
SEE PROFILE

THE JOURNAL OF PHYSICAL CHEMISTRY A

ARTICLE

pubs.acs.org/JPCA

Theoretical Study of the Crystal-Field Energy Levels and Two-Photon Absorption Intensities of Tb^{3+} in Cubic Host Lattices

Chang-Kui Duan[†,‡,§] and Peter A. Tanner[*,‡]

[†]College of Physics and Mathematics, Chongqing University of Post and Telecommunications, Chongqing, P.R. China

[‡]Department of Biology and Chemistry, City University of Hong Kong, Tat Chee Avenue, Kowloon, Hong Kong S.A.R., P.R. China

ABSTRACT: Published two photon excitation (TPE) intensities for the cubic elpasolite systems Cs_2NaTbX_6 (X = Cl, F) have been simulated by a calculation of two photon absorption (TPA) intensities which takes into account electric dipole transitions involving the detailed crystal-field structure of $4f^7 5d$ intermediate states, as well as the interactions of the $4f^7$ core with the d-electron. The intensity calculation employed parameters from an energy level calculation which not only presented an accurate fit, but also yielded parameters consistent with those from other lanthanide ions. The calculated intensities were used to confirm or adjust the previous assignments of energy levels, resulting in some minor revisions. Generally, the TPA intensity simulations were in better agreement with experimental data for the fluoride, rather than the chloride, system and possible reasons for this are given.

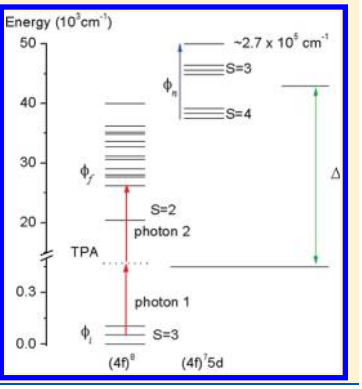

INTRODUCTION

This work presents calculations of the $4f^8$ crystal-field (CF) energy levels of Tb^{3+} in Cs_2NaTbX_6 (X = Cl, F) and utilizes the wave functions thereby obtained for the further calculations of intensities in the two-photon absorption (TPA) spectra of these crystals. Experimental two photon excitation (TPE) data have been recorded by Denning and co-workers in several detailed studies at temperatures down to 6 K from oriented crystals using polarized radiation and the use of a magnetic field.[1−6] Other studies of $Cs_2NaTbCl_6$ have utilized conventional one photon luminescence and absorption spectroscopy, as well as magnetic circular dichroism.[7−10]

We recognize that the results of CF calculations which indicate systematic trends of CF parameters (CFPs) throughout the lanthanide series not only serve to validate the correctness of the calculations, but also to throw light upon the physical meaning of the parameters.[11] Such calculations require representative, securely assigned energy level data sets so that the derived CFPs have less uncertainties. Some previous calculations have employed incorrect matrix elements, and we also find in the present study that a few assignments can be changed in order to provide a more accurate data set fitting.[12] Although semiempirical CF theory has been successful in the simulation of the energy levels of lanthanide ions (Ln^{3+}), it can be more useful if it can be used to predict, rather than explain, the positions and properties of the Stark levels. Whereas *ab initio*/first principle calculations have gained tremendous successes in various fields of materials science, and there are also some notable attempts for lanthanide materials,[13−16] it is not yet possible to perform calculations using these methods alone which can give a good comparison with experimental results down to the level of Stark splittings. Recently, Reid and co-workers[17] have proposed to combine *ab initio*/first principle calculations with the semiempirical CF effective Hamiltonian for energy level and intensity calculations and have demonstrated the method with an example for CF energy levels. Along these lines, it is important to obtain accurate CFPs from model systems to test the theoretical methods, and to elucidate the mechanisms of the contributions to those parameters.

The elpasolite host, Cs_2NaLnX_6, has the attractive property of providing sites of high symmetry (O_h molecular symmetry point group) for Ln^{3+}. The absorption spectrum for the transition from an initial state (usually the ground state or a low-lying excited state) to an excited state by the simultaneous absorption of two photons (two-photon absorption, TPA) can give complementary information to the one-photon absorption spectrum. The mechanism of TPA for Tb^{3+} is depicted in Figure 1 (refer also to the Theory section). TPA is usually extremely weak so the subsequent emission due to absorption is detected instead in the two-photon excitation (TPE) spectrum. The TPE studies using polarized radiation have been particularly powerful in the assignment of symmetry representations to crystal-field levels since stricter point group selection rules determine the intensities of electronic transitions between CF levels,[1] by comparison with the one photon electronic spectra of these cubic crystals. The one-color TPE studies also possess the advantage that high-lying Stark levels are accessible by using visible laser radiation, since the laser photon energy involved is only half of that for the terminal level. The spectra comprise pure electronic transitions and are mostly uncluttered by vibronic structure. By contrast, the one photon ultraviolet spectra tend to be very congested so that spectral assignments are frequently ambiguous.

Transition intensity calculations can be useful in checking the assignments of Stark levels, and also they serve to check the

Received: December 7, 2010
Revised: January 18, 2011
Published: February 22, 2011

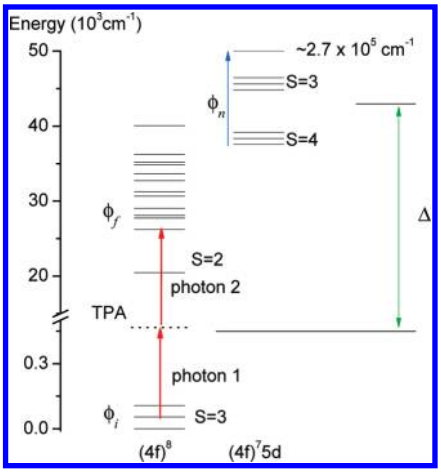

Figure 1. Schematic diagram of TPA of Tb^{3+} between $4f^8$ states. By absorbing two photons at the same time, Tb^{3+} is excited from the ground state or thermally activated state ϕ_i (crystal-field level of $^7F_6$) to various final states ϕ_f. The intermediate states ϕ_n contributed to the TPA transition intensities due to the product of the ED moments $\langle\phi_f|D_\sigma^{(1)}|\phi_n\rangle$ and $\langle\phi_n|D_\sigma^{(1)}|\phi_i\rangle$ weighted by the inverse of Δ, the energy difference between intermediate state and the average energy of the initial and final states. In this case, the ranges of energies of the states involved in the calculation are 0 to 100 cm^{-1} (ϕ_i), ~2×10^4 cm^{-1} to ~4×10^4 (ϕ_f), and ~3.5×10^4 cm^{-1} to 2.7×10^5 cm^{-1} (ϕ_n).

modeling accuracy when using the semiempirical CF Hamiltonian. The rare earth literature contains many calculations of the intensities of one-photon spectra, either based on the three-parameter Judd−Ofelt theory,[18] or on its extension to transitions between Stark levels.[19] TPA intensity calculations can certainly serve the same goal, and we have employed them to explore the properties of CF levels. However, there are very few calculations of TPA intensities in the literature, especially concerning the intensities of transitions between individual Stark levels. Most previous calculations adopted various approximations of intermediate states to avoid direct summation over many of these states. In particular, the intensity of the $^7F_6A_{1g} \rightarrow {}^5D_4A_{1g}$ transition of Tb^{3+} in $Cs_2NaTbCl_6$ has attracted previous attention[20−23] and highlighted the sensitivity of transition strengths to intermediate state energies and the minute eigenfunction mixing of states.[24]

The TPA calculation for CaF_2:Eu^{2+} is an example of a complete calculation utilizing intermediate states,[25] but the drastic variation of the line widths of the experimental peaks makes the comparison of calculated and observed TPA strengths less definite. Both this calculation (for Eu^{2+}) and our recent calculation on Gd^{3+}[26] concern ions with a half-filled 4f orbital, whose ground multiplet $^8S_{7/2}$ contains several (three for the O_h site) degenerate (for the purpose of optical spectroscopy) CF levels. However, the number of states identified by TPE for Eu^{2+} and Gd^{3+}[27,28] is very limited. By contrast, for Tb^{3+} in Cs_2NaTbF_6 and $Cs_2NaTbCl_6$, there have been more than 90 and 130 experimentally observed levels, respectively, in the one-photon and TPE spectra.[2,3] Furthermore, there are well-resolved TPE transitions not only from the ground state $^7F_6$ A_1, but also from the lowest-excited state $^7F_6$ T_1, due to thermal excitation. These types of transition obey different symmetry selection rules and are particularly informative for the assignments of irreducible representations (irreps) to CF levels. The crystals Cs_2NaTbF_6 and $Cs_2NaTbCl_6$ are closely related in many respects, but the differences in TPE intensities for many portions of the measured spectra are remarkable. Thus, it is essential to not only to make the comparison study of experiment with theory for each compound, but also to perform the comparison between theoretical results for the two systems.

The format of this study begins with brief directions to the relevant literature concerning the theory of two-photon calculations and the method of $4f^N$ energy level parametrizations, both of which are too extensive to cover herein. Then the revised energy level fittings and parameters are presented, and the extensive calculations of TPA intensities are listed. This is followed by an in-depth analysis of the experimental TPE spectra and the comparison of fluoride and chloride systems. Finally, some minor revisions to the energy level data sets are mentioned, and the limitations of the present study are highlighted.

THEORY

The general expression for the rate of TPA for the case of a one-color laser beam has been previously given[25] and applied to the CaF_2:Eu^{2+} system. Since Tb^{3+} is similar to Eu^{2+} in that the lowest excited electronic configuration is $4f^{N-1}5d$ ($N = 7$ for Eu^{2+} and 8 for Tb^{3+}), we follow ref 25 to include only the most important intensity contribution due to electric dipole radiation. The transition element M_{if} between the ground state and the final state for the case of a one-color laser beam is as follows

$$\sum_n \frac{\langle\psi_f|D_\sigma^{(1)}|\psi_n\rangle\langle\psi_n|D_\sigma^{(1)}|\psi_i\rangle}{hc(\bar{\nu}_f + \bar{\nu}_i)/2 - hc\bar{\nu}_n} \quad (1)$$

where $hc\bar{\nu}_i$, $hc\bar{\nu}_f$, and $hc\bar{\nu}_n$ are the energies for the initial, final, and intermediate (also referred to as virtual) states involved in the TPA process; and σ and $hc\bar{\nu}_1 = hc(\bar{\nu}_f - \bar{\nu}_i)/2$ represent the laser photon polarization and energy, respectively. This mechanism is subsequently abbreviated as ED-ED. The TPA line strength is then the squared modulus of expression 1. When using cm^{-1} and cm for the units of the energy denorminator and the position of electrons in the electric dipole moment, we obtain the unit for TPA line strengths as cm^6.

To avoid the arbitrariness in the choices of two-body correlation crystal-field parameters, we obtained the eigenvalues and eigenvectors of all the states in the $4f^8$ configuration using an adjustable quasi-free-ion empirical Hamiltonian with a site-symmetry adapted one-body CF Hamiltonian. A description of the parameters and their relative importance has been given elsewhere.[11]

Eigenvalues and eigenvectors of all the TPA intermediate states in the $4f^7$5d configuration were obtained using the extended empirical Hamiltonian,[29] which includes quasi-free-ion and one-body CF interactions in the $4f^7$ core, together with spin−orbit and crystal-field interactions for the 5d electron, and Coulomb interaction between the 4f and 5d electrons.[30,31] The same procedure as in ref 32 was used to assign the parameter values for the $4f^7$5d configuration. The parameters and their obtained values are listed in Table 1 with some further explanations. Note that, in the TPA intensity calculations, the summation over all $4f^7$5d virtual CF states was taken explicitly by following ref 25. This is in contrast to those calculations based on perturbation expansion by Judd and Pooler,[33] Downer,[34] and Burdick and Reid,[35,36] and calculations based on the neglect of f−d interactions.[37]

dx.doi.org/10.1021/jp111620e |J. Phys. Chem. A 2011, 115, 1922–1932

Table 1. Optimized Parameter Values for the Energy Levels of the $4f^8$ Configuration of Tb^{3+} in Cs_2NaTbX_6 (X = F, Cl)[a]

	$Cs_2NaTbCl_6$		Cs_2NaTbF_6		difference	
param	P(Cl)	Δ(Cl)	P(F)	Δ(F)	P(F) − P(Cl)	Δ
			$4f^8$			
E_{AVG}	68007	85	68578	73	571.6	112
F^2	88435	389	88800	178	365.6	427
F^4	63031	554	64240	437	1209.0	706
F^6	45027	433	47714	458	2686.3	630
ζ_{4f}	1697.3	3.2	1698.5	4.2	1.2	5.2
N_{expt}	130		93			
N_{param}	14		11			
σ	22.1		22.7			
δ	20.9		21.3			
			$4f^8$ and $4f^7$5d			
α	19.0	0.9	22.4	0.4	3.4	1.0
β	−568	36	−831		−262.8	
γ	1754	154	1309		−445.7	
T^2	105	40	291	55	185.6	68
T^3	40		40		0.0	
T^4	45		45		0.0	
T^6	−365		−365		0.0	
T^7	320		320		0.0	
T^8	139	46	231		92.2	46
M^0	4.26	0.29	3.24	0.37	−1.03	0.47
P^2	851	89	574	117	−276.3	147
B_4	1686	28	3251	34		
B_6	228	18	257	22		
			$4f^7$5d			
$F^2(f^6d)/F^2$	1.0613		1.0613			
$F^4(f^6d)/F^4$	1.0635		1.0635			
$F^6(f^6d)/F^6$	1.0683		1.0683			
$\zeta_{4f}(f^6d)/\zeta_{4f}$	1.0730		1.0730			
B_4(5d)	36500		45200			
E_{exc}	73600		78800			
η_{fd}	0.53		0.55			
ζ_{5d}	1185		1557			

[a] Restrictions adopted in the calculation are the following: $M^2 = 0.56M^0$, $M^4 = 0.38M^0$; $P^4 = 0.75P^2$, $P^6 = 0.5P^2$; $H_{cf}(4f) = B_4(4f)[C_0^{(4)}(4f) + (5/14)^{1/2}\{C_{-4}^{(4)}(4f) + C_4^{(4)}(4f)\}] + B_6(4f)[C_0^{(6)}(4f) - (7/2)^{1/2}\{C_{-4}^{(6)}(4f) + C_4^{(6)}(4f)\}]$; $H_{cf}(5d) = B_4(5d)[C_0^{(4)}(5d) + (5/14)^{1/2}\{C_{-4}^{(4)}(5d) + C_4^{(4)}(5d)\}]$. The deviations of the optimization are given in terms of $\sigma = [\Sigma_i(E_{calc}(i) - E_{expt}(i))^2/(N_{expt} - N_{param})]^{1/2}$ and $\delta = [(E_{calc}(i) - E_{expt}(i))^2/N_{expt}]^{1/2}$, where N_{expt} is the number of measured levels and N_{param} is the number of variable parameters. The columns P(X) and Δ(X) give the optimized values and their uncertainties obtained in the calculation (the parameters stated without uncertainties were fixed in the optimization). The column "difference" gives the difference of values between quasi-free-ion parameters for Tb^{3+} in the two hosts and their uncertainties, $\Delta = [\Delta(F)^2 + \Delta(Cl)^2]^{1/2}$. The parameters employed to calculate the $4f^7$5d energy levels used for the TPA calculations are also listed. All the parameters listed for $4f^8$ were also used for $4f^7$5d, and those not listed were assigned with the same values as for the $4f^8$ configuration. The Hartree−Fock values for the 4f−5d Coulomb interaction parameters [(in cm^{-1}): $F^2(fd) = 29\,795$, $F^4(fd) = 14\,347$, $G^1(fd) = 12\,247$, $G^3(fd) = 10\,508$, and $G^5(fd) = 8146$] were scaled by the factor η_{fd}. The parameter E_{exc} is the separation between the barycenters of the $4f^8$5d and $4f^8$ configurations, which was chosen to give the onset of the $4f^7$5d levels, as predicted in ref 32. The units of all energy parameters are cm^{-1}, and parameter ratios are dimensionless.

RESULTS AND DISCUSSION

Consistent and Well-Defined Quasi-Free-Ion Parameters for Tb^{3+} in $Cs_2NaTbCl_6$. Previous calculations for these systems have used the matrices of f^6 tensors with appropriate change of signs, instead of those for f^8. To obtain consistent F^k ($k = 2, 4, 6$) parameters, it is more accurate to employ the correct matrices for t_k ($k = 2-4, 6-8$) which contain, in addition to three-body contributions, some two-body contributions. These are different from the matrices of t_k for f^6 not only by sign. Thus, we use the proper matrices for the t_k tensors, in addition to the corrected matrices for m_k and p_k tensors.[12] All levels derived from TPE measurements (as well as the lower energy levels determined from one-photon spectroscopy) have been included in the energy level optimizations. The residues of optimization obtained here (ca. 22 cm^{-1}) are comparable with those from previous calculations.[2,3] However, the parameters are slightly different from previous results.[2,3,5] It is important that these

differences are taken into account, since the energies of CF levels are very sensitive to F^k values. The use of previous parameter values with the current corrected tensors give very different energies for many Stark levels.

Some comments are now made concerning the derived parameter values (Table 1) from the $4f^8$ energy level fittings of 130 levels for Cs_2NaTbF_6 and 93 levels for $Cs_2NaTbCl_6$. The Coulomb parameter F^2 for Tb^{3+} in Cs_2NaTbF_6 is similar to that in $Cs_2NaTbCl_6$. A more distinctive trend is found for F^4 and F^6, since the relevant differences are rather greater than parameter value uncertainties. It is also observed that the ligand distinction of the hexacoordination environment (F^- or Cl^-) upon F^k increases from $k = 2$ to $k = 6$. The obtained ratios for Coulomb parameters from our fittings [$F^4/F^2 = 0.713$ (Cl) or 0.723 (F); $F^6/F^2 = 0.509$ (Cl) or 0.537 (F)] are consistent with the ratios for Tb^{3+} in various hosts and with the ratios for lanthanide ions across the lanthanide series. The spin−orbit coupling interaction ζ_{4f} is essentially the same for the fluoride and chloride systems, considering that the difference in values is only 1.2, but the combined uncertainty is 5.2. Differences for T^2 and T^8 in the two hosts are also apparent for the two hosts, whereas other T^k parameters are similar. As expected, the CFPs turn out to be substantially larger for F^- than Cl^- ligands. The CF parameter $B_4(4f)$ (abbreviated to B_4) is also consistent with values for other lanthanide elpasolites,[11] although B_6 for Tb^{3+} in Cs_2NaTbF_6 is smaller than for other Cs_2NaLnF_6 systems. However B_6 is nearly an order of magnitude smaller than B_4. Other parameters were either constrained in the full or final stage of fitting due to extremely large uncertainties, so that comparisons cannot be meaningfully made.

The additional parameters for the $4f^75d$ electronic configuration, given at the lowest part of Table 1, were taken from previous calculations,[32] with E_{exc} adjusted to reflect the onset of the configuration.

The rationale for energy level data presentation in Table 2 is now explained. Since the CF splitting in $Cs_2NaTbCl_6$ is smaller than for the corresponding fluoride, and the energy levels from different $^{2S+1}L_J$ multiplets are less cluttered, the calculated levels in this host are labeled in the order of increasing energy, as given in column 1 (N) of Table 2 (except for levels 172−174). Then, the calculated levels for Cs_2NaTbF_6 are arranged with matching irreps (column 5, E_{calc}). The CF splitting in Cs_2NaTbF_6 is much larger, and many levels of different multiplets cross over, so that the levels with a larger label number from column 1 are not always higher in energies than their predecessors. The experimentally measured levels are assigned to the closest calculated levels of the appropriate symmetry. The original labels of measured levels for $Cs_2NaTbCl_6$[3] and Cs_2NaTbF_6[2] from the TPE studies are given in the columns N_{exp}. The lower energy levels of $^7F_6$ ($N = 4-6$), and ^7F_J ($J = 5...0$) ($N = 7-21$), were determined from one-photon spectra[10] and have been omitted from Table 2, although they were included in the energy level fittings.

TPA Line Strengths. TPE intensities were measured[2,3] for polarized radiation propagating along [100] and [110] directions at 10 and 40 K for Cs_2NaTbF_6, and at 10 and 25 K (except for the region from 36 150 to 36 550 cm^{-1} at 77 K) for $Cs_2NaTbCl_6$. At those temperatures, only the ground state A_1 (0 cm^{-1}) and the first two excited states T_1, T_2 (at 55, 107 cm^{-1} for Cs_2NaTbF_6, and at 34, 74 cm^{-1} for $Cs_2NaTbCl_6$) are appreciably thermally populated and thus give transitions in the measured TPE spectra. Since the polarization factors for one-beam TPA transitions transform as $A_1 + E + T_2$ (O_h), the absorption from A_1 is only allowed to excited A_1 (by A_1 operator), E (by E operator), and T_2 (by T_2 operator) CF levels. Absorption from T_1 is allowed to excited A_2 (by T_2 operator), E (by T_1 and T_2 operators), T_1 (by A_1, E, and T_2 operators), and T_2 (by E and T_2 operators) states, and from T_2 absorption is allowed to excited A_1 (by T_2 operator), E (by T_1 and T_2 operators), T_1 (by E and T_2 operators), and T_2 (by A_1, E, and T_2 operators) states. For transitions solely due to the A_1 operator, the intensities are polarization invariant; for transitions solely due to the E operator, the intensity for [110]-polarized light is $^1/_4$ of that for [100]-polarized light; and for transitions solely due to the T_2 operator, the intensity for [100] polarization is zero but is nonzero for [110]-polarized light. These selection rules provide useful information for the assignment of symmetry irreps to the excited CF states.

All of the TPA line strengths from the three lowest $^7F_6$ states to all excited states in the energy range from just above 20 000 cm^{-1} ($^5D_4$) to just below 41 200 cm^{-1} ($^5K_8$) have been calculated. In Table 2, only the line strengths for allowed transitions are listed, and the zero calculated line strengths for forbidden transitions are left blank for clarity. Since almost all of the experimentally observed transitions are from the first two levels (A_1 and T_1), we only list in Table 2 the line strengths for those transitions from these first two levels to the $^{2S+1}L_J$ multiplets measured by TPE spectra. For comparison with experimental data, the line strengths for TPA from the $^7F_6T_1$ must be weighted by the Boltzmann factor $\exp[-E(^7F_6T_1)/(k_BT)]$, equal to 0.138 (for Cs_2NaTbF_6 at 40 K), or to 0.141 (for $Cs_2NaTbCl_6$ at 25 K, except for the energy range 36 150−36 550 cm^{-1}, measured at 77 K and where the factor is 0.53). The 3-fold degeneracy of T_1 has been taken into account in the definition of line strengths and should not be multiplied again. The measured TPE intensities were not corrected for spectral response, so the values in Table 2 are normalized with respect to the strongest transition for each multiplet (i.e., each section in Table 2). Noting that the terminal multiplets only extend over a relatively narrow spectral range, the transition line strength ratios are well-approximated by measured relative intensities. Hence in the following discussion only the relative values of the calculated line strengths within each multiplet have been compared with measured ones. It is also noted that since the experimental data from Denning's studies[2,3] are TPE intensities, and the calculated line strengths are those for TPA, the values are comparable for a given multiplet term. The TPA and TPE intensities may not be comparable for TPA transitions from the electronic ground state to different excited multiplet terms, unless the nonradiative relaxation rate from the latter to the luminescent state ($^5D_4$) is fast. The transition strengths for individual multiplets are now discussed. The reference to specific CF levels utilizes the notation N (column 1 of Table 2), unless otherwise stated.

Multiplet $^5D_4$ (Levels 22−25). When comparing the $^5D_4$ measured relative intensities for the chloride and fluoride systems, the most striking difference is the relative strength for the A_1-A_1 transition, which is calculated to be more than 3 times stronger in $Cs_2NaLnCl_6$ than in Cs_2NaTbF_6.

The strongest experimentally observed transition for Cs_2NaTbF_6 is the one denoted by $N = 23$ (final state: $^5D_4$ T_1) and column 110b ([110], direction of the polarization of light; b, initial state $N = 2$, $^7F_1$ T_1). The calculated absolute line strength for this transition is 1.43×10^{-50} cm^6 (i.e., in Table 2, 1038 weighed by 0.138). Using this as reference, the transition $N = 1$ to $N = 24$ ($^7F_1A_1-{}^5D_4E$) under the same polarization

Table 2. Comparison of Calculated and Observed Energy Levels and TPA Line Strengths for Tb^{3+} in Cs_2NaTbF_6 and $Cs_2NaTbCl_6$[a]

state			Cs_2NaTbF_6			calcd		expt		calcd		expt		$Cs_2NaTbCl_6$			calcd		expt		calcd		expt	
N	SLJ	IR	N_{exp}	E_{calc}	E_{exp}	100a	110a	100a	110a	100b	110b	100b	110b	N_{exp}	E_{calc}	E_{exp}	100a	110a	100a	110a	100b	110b	100b	110b
1	$^7F_6$	A_1	1	11	0	—	—	—	—	—	—	—	—	1	−2	0	—	—	—	—	—	—	—	—
2	$^7F_6$	T_1	2	67	55	—	—	—	—	—	—	—	—	2	34	34	—	—	—	—	—	—	—	—
3	$^7F_6$	T_2	3	130	107	—	—	—	—	—	—	—	—	3	78	74	—	—	—	—	—	—	—	—
22	$^5D_4$	A_1	22	20 634	20 672	20	20	0.43	0.26					22	20 455	20 470	68	68	1	1				
23	$^5D_4$	T_1	23	20 696	20 711					496	1038	0.3	1	23	20 482	20 488					823	549	0.2	0.25
24	$^5D_4$	E	24	20 741	20 740	266	67	0.43	0.13		442	0.09	0.48	24	20 501	20 500	458	115	0.2	0.1		451	0.1	0.25
25	$^5D_4$	T_2	25	20 896	20 838		13		vw	372	303	w	w	25	20 586	20 553		14		0.05	159	137	0.12	0.12
26	$^5D_3$	A_2	26	26 377	26 383						100		no	26	26 198	26 219						190		w
27	$^5D_3$	T_2	27	26 453	26 454		99		0.2	25	734	vw	0.3	27	26 260	26 261		131	0.4	1	1108	487	0.4	0.3
28	$^5D_3$	T_1	28	26 500	26 494					1141	2863	0.6	1	28	26 291	26 284					6	4	1	1
29	$^5G_6$	T_2	30	26 581	26 561	0	3465		1	4505	1303	0.14	0.05	30	26 344	26 378		3621	0.6	1	4204	1822	vw	vw
30	$^5G_6$	A_1	29	26 560	26 554	1097	1097	0.46	0.68					29	26 352	26 372	885	885	vw	vw				
31	$^5G_6$	T_1	31	26 612	26 597					2338	7731	0.25	0.50	31	26 362						2942	11000	no	no
32	$^5G_6$	E	35	26 792		752	188	no	no		16		no	32	26 448	26 412	336	84	1.3	1.1		51		vw
33	$^5G_6$	T_2	36	26 839	26 854		1478		0.23	38	1684	no	no	33	26 495	26 467		1046	w	0.6	38	1107	vw	vw
34	$^5G_6$	A_2	37	26 910							1823		no	34	26 558							962	vw	w
35	$^5L_{10}$	E	32	26 629	26 618	345	86	0.72	0.16		83		no	35	26 681	26 685	513	128	vw	vw		40		no
36	$^5L_{10}$	T_2	33	26 640	26 653		44		0.13	948	250	0.33	0.09	36	26 689	26 694		349	0.5	1.3	548	355	0.03	0.06
37	$^5L_{10}$	A_2	34	26 662							216	no	no	37	26 706	26 722						638		vw
38	$^5L_{10}$	T_2	38	27 142	27 140		9		no	2	162	vw	w	38	26 943	26 925		1		vw	3	110		vw
39	$^5L_{10}$	T_1	39	27 221	27 211					517	251	0.43	0.29	39	26 993	26 975					338	161	vw	vw
40	$^5L_{10}$	A_1	40	27 445	27 433	49	49	0.07	0.07					40	27 093	27 086	19	19	5	5				
41	$^5L_{10}$	T_1	41	27 645	27 640					455	177	0.02	0.007	41	27 237	27 230					385	215	vw	vw
42	$^5L_{10}$	E	42	27 723	27 705	645	161	0.14	0.036		371		0.007	42	27 276	27 271	180	45	vw	vw		37	vw	vw
43	$^5L_{10}$	T_2	44	27 835			9		no	5	38	no	no	43	27 316	27 318		16		0.08	14	30	vw	vw
44	$^5G_5$	E	43	27 815	27 854	2326	582	1	0.25		1805		0.03	44	27 687	27 729	3416	854	1	0.3		2200	0.6	2
45	$^5G_5$	T_1	45	27 857	27 906					4558	1195	0.15	w	45	27 719	27 737					5443	1373	0.12	0.15
46	$^5G_5$	T_1	46	28 034	28 015					637	1317	w	w	46	27 770	27 775					795	722	0.12	0.08
47	$^5G_5$	T_2	47	28 072	28 055		636		0.05br	1134	554	w	w	47	27 800	27 790		413		0.5	1289	420	0.08	0.15
48	$^5D_2$	T_2	50	28 375	28 358		197		0.7	124	141	0.08	vw	48	28 117	28 110		139		0.13	144	317	0.2	0.4
49	$^5D_2$	E	52	28 496	28 506	373	93	1	0.25		802		0.5	49	28 200	28 200	712	178	1	0.25		788		0.6
52	$^5G_4$	A_1	51	28 460	28 421	43	43	w	w					50	28 236	28 206	29	29	0.05	0.05				
53	$^5G_4$	T_1	57	28 630	28 680					325	179	vw	vw	53	28 301	28 270					78	49	w	w
54	$^5G_4$	T_2	54	28 477	28 531		407		1	871	1290	vw	0.25	54	28 308	28 323		368		1	768	1044	wbr	wbr
55	$^5G_4$	E	56	28 696										55	28 335		78	19	no	no		37	no	no
50	$^5L_9$	T_1	48	28 329	28 333					31	34	w	w	51	28 214	28 216					73	181	0.5	0.6
51	$^5L_9$	T_2	49	28 348	28 353		180		1.5	72	110	0.02		52	28 233	28 233		89		1.2	90	23	w	w
56	$^5L_9$	E	53	28 525	28 553	373	93	0.75	0.2		396		no	56	28 382	28 388	4	1	0.01	vw		53		no
57	$^5L_9$	T_1	55	28 539						43	83	no	no	57	28 394	28 393					7	21	vw	w
58	$^5L_9$	A_1	58	28 794	28 811	3	3							58	28 566	28 560	1	1						
59	$^5L_9$	T_1	59	28 920	28 954					28	77	0.02	0.06	59	28 620	28 616					17	76	w	0.3
60	$^5L_9$	T_2	60	28 993	29 000		1	vw	vw	264	86	no	no	60	28 659	28 656		1	w	w	129	108	w	w
61	$^5L_9$	A_2	61	29 056	29 037						75	0.2	0.1	61	28 692	28 730					0	70		vw
62	$^5G_3$	T_2	63	29 159	29 179		1	vw	0.3	5	22	0.02	0.1	63	28 984	28 983		2		0.5	48	30	vw	vw
63	$^5G_3$	T_1	64	29 182	29 194					42	14	0.15	0.1	62	28 984	28 960				0	27	7	w	w
64	$^5G_3$	A_2	65	29 173							149			64	29 011	29 033						19		vw
65	$^5L_8$	A_1	68	29 335	29 337	3	3	0.3	0.3					65	29 045	29 052	1	1	1	1				
66	$^5L_8$	T_1	67	29 322	29 308					69	27	0.05	0.05	66	29 050	29 056					24	32	w	w
67	$^5L_8$	E	62	29 191	29 128	6	2	vw	vw		8			67	29 055	29 059	19	5	w	w		5	w	w
68	$^5L_8$	T_2	66	29 258	29 298		8		0.01	126	194	0.015	0.017	68	29 068	29 095		3		w	4	4		
69	$^5L_7$	T_1	71	29 424						136	46	0.01br	vvw	69	29 214	29 211					9	11	0.01	0.01

dx.doi.org/10.1021/jp111620e |J. Phys. Chem. A 2011, 115, 1922–1932

Table 2. Continued

state			Cs_2NaTbF_6			calcd		expt		calcd		expt		$Cs_2NaTbCl_6$			calcd		expt		calcd		expt	
N	SLJ	IR	N_{exp}	E_{calc}	E_{exp}	100a	110a	100a	110a	100b	110b	100b	110b	N_{exp}	E_{calc}	E_{exp}	100a	110a	100a	110a	100b	110b	100b	110b
70	$^5L_6$	T_2	69	29 361	29 360		26		0.01br	8	2	no	no	70	29 268	29 272		4		vw	82	47	vw	vw
71	$^5L_7$	A_2	72	29 516							3		no	71	29 296							62		
72	$^5L_6$	E	70	29 390	29 425	10	3	0.1	0.03		1		vvw	72	29 310	29 312	18	4	0.01	0.002		9		
73	$^5L_6$	T_2	73	29 682	29 673		25		vvw	61	22	0.05br	0.01br	73	29 445	29 451		14		0.05	88	64	vw	0.01
74	$^5L_8$	E	74	29 780	29 751	82	20	vw	vw		34		0.01	75	29 447	29 465	1		vw			4		vw
75	$^5L_8$	T_2	75	29 870	29 866		21		vw	57	43	vw	vw	76	29 451	29 467		68		vw	65	17	vw	vw
76	$^5L_8$	T_1	76	29 924	29 930					8	74	0.15	0.03	74	29 466			0			20	90	no	no
77	$^5L_7$	T_2	78	29 990	29 985		178		0.7br	14	94	vvw	vw	78	29 592	29 573		71		w	105	114	vw	vw
78	$^5G_2$	E	77	29 981	29 957	55	14	1	0.2		7		no	77	29 604	29 553	116	29	vw	vw		1		
79	$^5L_7$	T_1	79	30 130	30 127					259	77	0.05	vvw	79	29 669	29 662					321	117	0.01	0.005
80	$^5L_7$	T_2	80	30 146	30 144		36		0.01br	110	48	no	no	80	29 717	29 697		19		0.01br	85	22	vw	vw
81	$^5L_7$	E	81	30 217	30 215	117	29	0.03br	vwbr		64		no	81	29 737	29 727	59	15	0.005	0.002		80		vvw
82	$^5L_6$	A_2	82	30 220							13			82	29 797	29 797						18		vvw
83	$^5L_6$	T_2	83	30 409	30 412		58		0.05	252	82			83	29 923	29 917		82		0.005	152	43	vvw	vvw
84	$^5L_6$	T_1	84	30 468	30 470					75	149	vw	vw	84	29 964	29 964					62	202	0.005br	0.005br
85	$^5L_6$	A_1	85	30 533	30 518	15	15	0.03	0.03					85	30 002	30 001	13	13	0.01	0.01				
86	$^5D_1$	T_1	86	30 927	30 946					515	339	0.05	0.1	86	30 648	30 652					452	189	no	no
87	$^5H_7$	T_1	87	31 522	31 516					1880	956	0.25	0.2	87	31 249	31 226					2645	1247	0.2	0.15
88	$^5D_0$	A_1	89	31 539	31 538	2	2	0.5	0.5					89	31 257	31 256	1	1	vvw	0.012				
89	$^5H_7$	E	88	31 537	31 531	1127	282	1	0.25		89		no	88	31 264	31 247	1663	416	1	0.3		215		
90	$^5H_7$	T_2	90	31 568	31 564	0	299	0.1	0.3	1231	572	0.07	0.05	90	31 284	31 272		512		0.12	2059	986	0.1	0.05
91	$^5H_7$	A_2	91	31 672							289		no	91	31 367							551		
92	$^5H_7$	T_2	92	31 819	31 836		12	0.07		1	12	no	no	92	31 426	31 448		69	vw			29		
93	$^5H_7$	T_1	93	31 863						239	109	no	no	93	31 450	31 479					448	307	w	w
94	$^5H_6$	A_1	94	33 037	33 007	65	65	0.15	0.15					94	32 783	32 732	43	43	0.8	0.8				
95	$^5H_6$	T_1	95	33 060	33 045					278	2225	0.1	0.2	95	32 794	32 758					254	2723	0.3	0.3
96	$^5H_6$	T_2	96	33 089			1070	0.2	1	266	94	0.1	0.05	96	32 809	32 789		1412		1	106	28		
97	$^5H_6$	A_2	97	33 208	33 242						935		vw	97	32 831	32 823						1175		w
98	$^5H_6$	T_2	98	33 273	33 298		51		no	593	929	vw	vw	98	32 907	32 934		1		0.04	1024	1177	0.03br	0.05br
99	$^5H_6$	E	99	33 286	33 309	389	97	0.1	w		19		no	99	32 915	32 945	500	125	0.02	vw		13		0.03br
100	$^5H_5$	T_1	100	33 899	33 877					721	267	vw	0.01	100	33 674						721	295	no	no
101	$^5H_5$	E	101	33 929	33 918	418	104	0.05	vw		457	vw	0.06	101	33 690	33 659	414	104	w	w		341		
102	$^5H_5$	T_2	102	34 098	34 083		523	0.2	1.0	428	213	0.1	0.05	102	33 730	33 730		367	0.7	1	678	262		
103	$^5H_5$	T_1	103	34 117						67	389	no	no	103	33 768	33 799					14	247	w	w
104	$^5H_4$	T_2	104	34 484	34 456		50	0.3	1	28	168	w	0.15	104	34 246			26		w	15	98		
105	$^5H_4$	T_1	105	34 672	34 652					192	186	no	no	106	34 320	34 331					35	55	0.1	0.1
106	$^5H_4$	E	106	34 698	34 683	18	4	0.7	0.25		56	w	0.15	105	34 327	34 307	0.32	0.08	0.002	0.0005	0	30		
107	$^5H_4$	A_1	107	34 760	34 798	4	4	w	w					107	34 362	34 406	6	6	1	1				
108	$^5F_5$	T_2	109	35 014			596			3702	1185			109	34 720	34 760		743		0.25	3602	1205	0.1	0.04
110	$^5F_5$	T_1	110	35 082						599	640			110	34 770	34 800					108	745	0.15	0.1
111	$^5F_5$	E	111	35 160		1900	475				825			111	34 820	34 822	2194	548	1	0.4		1017		vw
112	$^5F_5$	T_1	112	35 191						2753	726			112	34 829	34 840					3951	992	0.12	0.1
109	$^5H_3$	A_2	108	34 943							5			108	34 744							2		no
113	$^5H_3$	T_2	113	35 262			34			38	149			113	34 884			35		no	122	90	no	no
114	$^5I_8$	T_2	114	35 305			205			5	259			114	34 975	34 960		170		0.25	49	256	w	w
115	$^5I_8$	E	117	35 356		44	11				122			116	35 016		379	95	no	no		361		no
116	$^5H_3$	T_1	116	35 356						47	73			118	35 017	34 972					159	52	0.2	0.2
117	$^5I_8$	A_1	115	35 355		13	13							117	35 026	34 967	8	8	1	1				
118	$^5H_3$	T_1	118	35 451						724	286			115	35 034						125	32		
119	$^5I_8$	T_2	119	35 453			348			1223	803			120	35 052	35 091		345		0.015	1050	815	vw	vw
120	$^5I_8$	E	120	35 454		918	230				360			119	35 076	35 090	248	62	0.1	w		250		vw
121	$^5I_8$	T_1	121	35 505						465	174			121	35 077						417	271	no	no

dx.doi.org/10.1021/jp111620e |J. Phys. Chem. A 2011, 115, 1922–1932

Table 2. Continued

state			Cs_2NaTbF_6			calcd		expt		calcd		expt		$Cs_2NaTbCl_6$			calcd		expt		calcd		expt	
N	SLJ	IR	N_{exp}	E_{calc}	E_{exp}	100a	110a	100a	110a	100b	110b	100b	110b	N_{exp}	E_{calc}	E_{exp}	100a	110a	100a	110a	100b	110b	100b	110b
122	$^5F_4$	T_2	122	35 560			79			1228	394			122	35 185			257		no	1302	706	no	no
123	$^5F_4$	E	123	35 680		559	140				284			123	35 258		768	192	no	no		459	no	no
124	$^5F_4$	T_1	124	35 748						601	260			124	35 294	35 273					867	383	0.3	1
125	$^5F_4$	A_1	125	35 792		25	25							125	35 315		14	14	no	no				
126	$^5F_3$	A_2	126	36 393							9			126	36 233	36 233						9	vw	0.1
127	$^5F_3$	T_2	127	36 547			46			35	49			127	36 340	36 310		36	0.6	1	20	53	0.2	0.25
128	$^5F_3$	T_1	128	36 642						31	32			128	36 392						23	19	no	no
129	$^5I_7$	E	129	36 835		3	1				0.03			129	36 476	36 510	9	2	1	0.5	0	2	0.5	1
130	$^5I_7$	T_1	130	36 843						18	7			130	36 480	36 518					10	11	0.7	0.7
131	$^5I_7$	T_2	131	36 871			0.3			8	2			131	36 495			3		no	1	3	no	no
132	$^5I_7$	A_2	132	36 884							9			132	36 528	36 527						22		1
133	$^5I_7$	T_2	133	36 948			2			29	8			133	36 550			0.003			39	10		
134	$^5I_7$	T_1	134	37 018			0			2	3			134	36 568						1	1		
162	$^5G_6$	E	162	40 262		157	39				19			162	40 035	40 045	140	35	w	w	0	18		no
163	$^5G_6$	T_2	163	40 280			40			630	681			163	40 036	40 050	0	188		1	985	917	w	w
164	$^5K_6$	A_1	165	40 432		20	20							164	40 132		53	53	no	no				
165	$^5K_6$	T_1	166	40 446						93	1801			165	40 133						182	2747	no	no
166	$^5G_6$	A_2	164	40 412							407			166	40 138						0	527	no	no
167	$^5K_6$	T_2	167	40 452			1099			630	160			167	40 140	40 156		1350	0.15	0.4	594	151	w	w
168	$^5K_8$	T_2	168	40 796			52			30	18			168	40 501	40 481		40	0.15	0.2	0	12		no
169	$^5K_8$	E	169	40 829		47	12				75			169	40 516	40 496	0.4	0.1	0.15	0.05	0	50		
170	$^5K_8$	T_1	170	40 835						57	113			170	40 529						6	63		
171	$^5K_8$	T_2	171	41 019			17			0	4			171	40 610	40 633		4		vw	8	14		
172	$^5K_8$	A_1	174	41 198		23	23							174	40 702	40 729	10	10		0.7			no	no
173	$^5K_8$	T_1	173	41 184						41	454			172	40 703	40 727			1		15	227	no	no
174	$^5K_8$	E	172	41 183		18	4				0.002			173	40 706		1	0.25			0	0.4		

[a] The column block "state" lists the sequence of the calculated levels (N), with respect to $Cs_2NaTbCl_6$; the major $^{2S+1}L_J$ component of the wavefunction (mult); and the O_h point group irreducible representation (IR) of the level, with the subscript g (omitted) throughout. The column block "Cs_2NaTbF_6" lists the numerical label of each level in the measured spectra[2] (N_{exp}) together with the calculated (E_{calc}) and measured[2] (E_{expt}) energies for the level. The calculated and measured TPA line strengths for [100]-polarized light and [110]-polarized light are given in the last eight columns of this block. This arrangement is similar for the third column block "$Cs_2NaTbCl_6$". The columns with the letter "a" and "b" denote that the TPA absorptions are from the ground state $^7F_6A_1$ and first thermally-excited state $^7F_6T_1$, respectively. Experimental values for TPE intensities (columns "expt") are measured from the heights of the lines in the literature TPE spectra.[2,3] Since the spectra were not corrected for response in different energy ranges, the intensity for the strongest peak in each section (row block, with the last energy level of the block underlined) is usually normalized to 1. A value followed by "br" means the peak is very broad, "w" means the height cannot be measured from the spectra but is expected to be about, or weaker than, 0.1 times the peak designated with value "1" in the block. Similarly, "vw" and "vvw" are similar to or weaker than 0.01 and 0.001 times of the peak designated with value "1" in the block, respectively. The "no" denotes that the peak was not observed in the experimental TPE spectra. Calculated line strengths are given in units of 10^{-52} cm^6, and blanks mean the values are zero due to selection rules. The calculated line strengths for ground and first thermally excited states need to be multiplied by Boltzmann factor $\exp(-E/k_BT)$, which, for Cs_2NaTbF_6, equals 1 for ground and equals 0.138 (40 K) for the first thermally excited states. For $Cs_2NaTbCl_6$, this equals 1 for the ground state and 0.141 (25 K) or 0.53 (77 K, for the energy range 36 150−36 550 cm^{-1}) for the first thermally excited states.

(column 110a) is overestimated by a factor of 3.6 [67/(143 × 0.13)], while the N = 1 to N = 22 transition ($^7F_1A_1$−$^5D_4A_1$) is underestimated by a factor of 3.1 (100a) or 1.9 (110a). The experimental intensity variation of the A_1−A_1 transition with polarization direction indicates that the actual effective incident light for the two polarizations may be different due to some reason, such as scattering, and this puts a constraint on the low limit of uncertainty of the measured intensities. A check of polarization leakage is also afforded by the ratios of intensities of A_1−E transitions in the two polarizations (theoretically 0.25). The nonzero measured value for the strictly forbidden transition N = 2 to N = 24 ($^7F_1T_1$−^5D_4E) under [100]-polarized light, which further indicates that there is polarization leakage. Other transitions in this multiplet are very well calculated in that the relative values are correctly predicted within the uncertainties for the measured intensities. The discrepancies between observation and calculation mentioned above may appear to be quite large, but this is partially due to the fourth power dependence of TPA line strengths on the ED moment. An overestimation of the moment by 1.5 times would result in an overestimate of TPA line strength by more than 5.06 times.

The predictions for $Cs_2NaLnCl_6$ follow similar trends, but with slightly more errors. The N = 1 to N = 22 (A_1−$^5D_4A_1$) transition is underestimated by a factor of 4.5, and N = 1 to N = 24 (A_1−$^5D_4$ E) is overestimated by a factor of 3.8 or 7 by comparison with the N = 2 to N = 23 (T_1−$^5D_4T_1$) transition.

Multiplet $^5D_3$ (Levels 26−28). This multiplet splits into A_2 + T_2 + T_1 CF levels, and there is only one (T_2) allowed TPA from the ground state (A_1). The measured TPA intensities for $^7F_6$−$^5D_3$ are quite similar for the systems, except that, for

Cs_2NaTbF_6, the absorption from $N = 2$ to $N = 26$ ($^7F_6T_1 - {}^5D_3A_2$) is much weaker and not observed in the printed spectra.

The strongest transition for Cs_2NaTbF_6 is from $N = 2$ to $N = 28$ ($T_1 - T_1$) under [110]-polarized incident light, for which the calculated absolute line strength is 395×10^{-52} cm^6. The measured relative intensities of other transitions are 0.6 for $N = 2$ to $N = 28$ (100b), 0.3 for $N = 2$ to $N = 27$ (110b), and 0.2 for $N = 1$ to $N = 27$ (110a), compared with calculated relative intensities 0.4, 0.26, and 0.25, respectively. There are two more allowed transitions, $N = 2$ to $N = 26$ (110b) and $N = 2$ to $N = 27$ (100b), with observed (calculated) relative intensities: not observed (0.03) and very weak (0.01), respectively. Thus, the calculated relative intensities agree with measured ones within a factor of 1.5, and this can be considered as very good, considering the various uncertainties in the measurement (such as systematic uncertainties and neglect of line width differences) and the sensitivity of the calculated intensities to small deviations of the ED moment.

The strongest transition for $Cs_2NaTbCl_6$ at 10 K is from $N = 1$ to $N = 27$ under [110]-polarized incident light (relative intensity = 1.0). The same transition under [100]-polarized incident light is strictly forbidden but was observed with a relative intensity of 0.4, presumably due to polarization leakage to the [110] direction. The relative intensities for transitions from $N = 2$ to $N = 27$ are measured as 0.4 (100b) and 0.3 (110b), and calculated as 1.2 (100b) and 0.52 (110b).

A large difference was found between the calculated intensities for the TPA transitions $N = 2$ to $N = 28$ for $Cs_2NaTbCl_6$ and Cs_2NaTbF_6, although the measured TPE intensities are similar. One explanation rests in different $^5G_6$ eigenvector mixing into $^5D_3$ calculated for the two cases. The calculation herein shows that the wave function of $N = 28$ contains about 24% $^5G_6$ for the fluoride but no more than 1% $^5G_6$ for the chloride system. For $Cs_2NaTbCl_6$, the TPA intensities for this case (T_1 $^7F_6 - {}^5D_3T_1$) were measured to be comparable with the reference transition in this multiplet (Table 2), but are calculated to be 0.0065 (100b) and 0.0043 (110b) in relative intensities. The next-higher T_1 level, $N = 31$, is predicted to have tremendous TPA line strengths from $N = 2$, but these transitions were not observed in the spectra. It is therefore possible that the observed T_1 level $N = 28$ actually corresponds to the calculated $N = 31$ with energy deviation -78 cm^{-1}. (We have not made this change.) Alternatively, and more probably, ~10−30% mixing of $^5G_6T_1$ into $^5D_3T_1$ can improve the calculated TPA intensities for $N = 2$ to $N = 28$.

Multiplet $^5G_6$ (Levels 29−34). This multiplet splits into $A_1 + A_2 + E + T_1 + 2T_2$ levels. The TPA intensities of transitions from $N = 1$ are much stronger than for $^5D_3$. Some experimental assignments for $Cs_2NaTbCl_6$ appear problematic and were made with reference to data other than TPE relative intensities. The $N = 24$ (A_2) CF level is unassigned for both the chloride and fluoride systems.

For Cs_2NaTbF_6, the strongest observed transition for this multiplet was assigned to $N = 1$ to $N = 29$ (110a), whose calculated absolute line strength is 3.47×10^{-49} cm^6. This is taken as the reference transition for the measurement of intensity ratios. The transition from $N = 2$ to $N = 29$ is allowed by E and T_2 operators, and so the ratio between two polarizations is not constrained. The measured relative intensities for these transitions are 0.14 (100a) and 0.05 (110a), compared with the calculated values 0.18 (100a) and 0.05 (110a). The transition from $N = 1$ to $N = 30$ is allowed only by the A_1 operator and is expected to be constant for (100a) and (110a) polarized light. However, the measured relative intensities are different: 0.46 (100a) and 0.68 (110a), compared with the calculated value 0.32. The transition from $N = 2$ to $N = 31$ is allowed by A_1, E, and T_2 operators so that the (100b)/(110b) ratio is not constrained either. The measured relative intensities are 0.25 (100b) and 0.5 (110b), compared to calculated values of 0.09 (100b) and 0.31 (110b), respectively. The transition from $N = 1$ to $N = 33$ is only allowed by the T_2 operator and hence is only allowed by [110]-polarized light. The relative intensity is measured (calculated) to be 0.23 (0.42). The agreement between calculated and measured relative intensities is thus good.

The $N = 1$ to $N = 29$ ($^7F_6A_1 - {}^5G_6T_2$) transition in [110] polarization is chosen as the reference for ease of comparison in the case of $Cs_2NaTbCl_6$. Selection rules imply that this transition is expected to exhibit zero intensity in [100] polarization, but in fact it is observed that relative intensity 0.6 could be due to polarization leakage. The strongest observed transition corresponds to the TPA transition $N = 1$ to $N = 32$ (^5G_6E) with the measured relative intensities 1.3 (100a) and 1.1 (110a). The relative intensities of these bands are calculated to be 0.093 (100a) and 0.023 (110a), respectively (i.e., 14−45 times weaker than observed), and their polarization dependence deviates considerably from that expected for an $A_1 - E$ transition at an O_h site, since the intensity for [110] polarization is a quarter of that for [100]. Another observed strong transition is $N = 1$ to $N = 33$ (110a) with measured (calculated) relative intensity 0.6 (0.3). Other transitions are both observed and calculated to be much weaker, and a definite comparison cannot be made.

Two weak bands are observed at 10 K for $Cs_2NaTbCl_6$ at ~26 494, 26 507 cm^{-1}. The first presumably corresponds to the moiety mode ν_5 (123 cm^{-1}) [or ν_2 (233 cm^{-1})] in conjunction with $^5G_6$ A_1 (26372 cm^{-1}) [or $^5D_3$ T_2 (26261 cm^{-1})]. The second band at 26 507 cm^{-1} may correspond to ν_5 based upon $^5G_6T_{2a}$, or the 45 cm^{-1} lattice mode based upon $^5G_6T_{2b}$. There is therefore no evidence for the assignment of the $^5G_6A_2$ level since these features cannot be associated with T_1 hot bands.

Multiplet $^5L_{10}$ (Levels 35−43). This multiplet splits into $A_1 + 2T_1 + 2E + 3T_2 + A_2$ CF levels. The common features for the two systems are that the measured TPE peaks are mostly very weak and the calculated ED−ED contributions are much weaker than those associated with the overlapping (for Cs_2NaTbF_6) or neighboring (for $Cs_2NaTbCl_6$) multiplets $^5G_6$ and $^5G_5$. The most striking difference in the chloride and fluoride TPE spectra is that the strongest transition in Cs_2NaTbF_6 is from the A_1 ground state to the first E level of the multiplet, whereas the strongest for $Cs_2NaTbCl_6$ is from the ground state to the A_1 level of the multiplet. As mentioned, the TPA of this multiplet is confused with that of $^5G_6$, so that the measured relative intensities are given using the same reference transition as for $^5G_6$, i.e., $N = 1$ to $N = 29$ (110a).

In the case of Cs_2NaTbF_6, almost all of the observed bands with intensities of ~0.1 or larger are underestimated in the calculation. In detail, the measured (calculated) relative intensities are the following: $N = 1$ to $N = 35$, 0.72 (0.1) in (100a) and 0.16 (0.025) in (110a); $N = 1$ to $N = 36$, 0.13 (0.013) in (110a); $N = 2$ to $N = 36$, 0.33 (0.04) in (100b) and 0.09 (0.01) in (110b); $N = 2$ to $N = 39$, 0.43 (0.02) in (100b) and 0.29 (0.01) in (110b); polarization independent $N = 1$ to $N = 40$, 0.07 (0.014); but $N = 1$ to $N = 42$, 0.14 (0.19) in (100a) and 0.036 (0.047) in (110a).

Similarly, for $Cs_2NaTbCl_6$, the calculated intensities of features are underestimated, and the most striking example concerns the polarization independent $N = 1$ to $N = 40$ (A_1-A_1) transition, where the measured (calculated) intensities are 5 (5×10^{-3}) relative to the reference transition $N = 1$ to $N = 29$ in (110a).

The small calculated values for almost all of these peaks indicate there are other contributions which become relatively important when the direct ED−ED contribution turns out to be very weak. One possible contribution is due to low-lying intermediate virtual states of the product of the $4f^7$ core with a linear combination of ligand orbitals/conduction band orbitals which transform similar to the components of the 5g ($l = 4$) orbital of Tb^{3+}. Another possible contribution is the dynamic coupling mechanism,[38] which is expected to be more important for $Cs_2NaTbCl_6$ than for Cs_2NaTbF_6.

Multiplet $^5G_5$ (Levels 44−47). This multiplet splits into $E + 2T_1 + T_2$ CF levels. TPA from the ground state is only allowed to the E and T_2 levels, and hence, the low temperature spectrum is expected to be dominated by two peaks. The A_1-T_2 ($N = 1$ to $N = 47$) peak is only slightly weaker than the A_1-E ($N = 1$ to $N = 44$) peak in $Cs_2NaTbCl_6$, but much weaker in the case of Cs_2NaTbF_6. The two T_1 levels were identified from hot band transitions.

The strongest transition for Cs_2NaTbF_6 is also the $N = 1$ to $N = 44$ (A_1-E) transition involving the E irrep symmetry TPA operator. The measured polarization dependence exactly matches the symmetry constraint. The measured (calculated) intensities of hot transitions are the following: $N = 2$ to $N = 44$ (T_1-E), 0.03 but broad (0.11) in (110b); $N = 2$ to $N = 45$, 0.15 (0.27) in (100b) and weak (0.067) in (110b). The transition operators for these two transitions both transform as T_2. The peak height of the transition $N = 1$ to $N = 47$ is measured (calculated) to be 0.05 (0.27) in (110a), but it is more than 5 times broader than the reference transition. Some other transitions are observed weak and are calculated to be weak also.

Using $N = 1$ to $N = 44$ (A_1 to E) as reference for $Cs_2NaTbCl_6$, then the measured (calculated) relative intensity is 2 (0.09). Since the $N = 2$ to $N = 44$ (T_1-E) transition is linked only by the T_2 operator, the TPA is only allowed under [110]-polarized light. The $N = 1$ to $N = 47$ (A_1-T_2) transition is also linked only by the T_2 operator with measured (calculated) relative intensity 0.5 (0.12) in (110a). Hence the agreement with experiment for the calculation concerning $Cs_2NaTbCl_6$ is not as good as for Cs_2NaTbF_6.

Multiplet $^5D_2$ (Levels 48, 49). The multiplet $^5D_2$ splits into $E + T_2$ CF levels, and transitions to both states are allowed by TPA from the electronic ground state. The regions between 28 100 and 28 400 cm^{-1} in $Cs_2NaTbCl_6$, and between 28230 and 28700 cm^{-1} in Cs_2NaTbF_6, are congested, but fairly complete assignments were given, except for some weak bands at and above 28 230 cm^{-1} in the fluoride spectrum. The observed relative intensity for $N = 1$ to $N = 48$ (A_1-T_2) in (110a) is much weaker, compared with transitions to neighboring multiplets, in $Cs_2NaTbCl_6$ than in Cs_2NaTbF_6. However, the $^5D_2$ relative transition intensities and polarization dependences are well-predicted for both systems. Whereas the (T_{2g} symmetry) feature at ~28 270 cm^{-1} in Cs_2NaTbF_6 may be assigned to the vibronic transition 362 (ν_2 e_g) + 27 906 (T_1), the assignment of the lower energy band at ~28 230 cm^{-1} is unclear.

Multiplet $^5G_4$ (Levels 52−55). The eigenvectors of overlapping states in the regions of the multiplet terms $^5G_4$, $^5D_2$, and $^5L_9$ are appreciably mixed so that in some cases herein the dominant term differs from that in the published energy level tabulations.[2,3] The multiplet $^5G_4$ splits into $A_1 + E + T_1 + T_2$ CF levels. The assignments given are tentative in some cases, partly due to band congestion and resonances with vibronic structure. For $Cs_2NaTbCl_6$, the A_1, T_1, and T_2 levels were assigned. A weak E symmetry band was assigned to the transition $N = 1$ to $N = 56$, although this band is calculated to be about 20 times weaker than that corresponding to $N = 1$ to $N = 55$.

For Cs_2NaTbF_6, the assignments of levels 52 (A_1) and 53 (T_1) were more straightforward. There are three E symmetry bands in this region, at 28 506, 28 517, and 28 553 cm^{-1}, and the first of these has been associated with $N = 1$ to $N = 49$, ^5D_2E. The 28 553 cm^{-1} band was assigned to $N = 1$ to $N = 55$ ^5G_4E, but the deviation from calculation is then −143 cm^{-1}. We prefer to assign this band to $N = 1$ to $N = 56$ ^5L_9E, which is calculated to be stronger. This leaves the weak E-type peak at 28 517 cm^{-1} unassigned. Although numerically feasible, this band cannot be assigned to a combination involving the participation of an ν_1a_{1g} (or a ν_5t_{2g} phonon) with a suitable electronic transition because in each case the symmetry would not be E-type. The calculated energy of ^5G_4E is 28 696 cm^{-1}, and there is a very weak, unassigned E-type peak[2] at 28 720 cm^{-1} which could correspond to $N = 1$ to $N = 55$, but this assignment has not been included in Table 2. The assignment of the $^5G_4T_2$ state of Cs_2NaTbF_6 at 28 531, 28 546 cm^{-1} is also problematic because two sets of transitions were associated with this state, with the explanation given that a resonance occurs between electronic and vibronic states. In fact, from the frequencies of ν_1 and ν_5, combination bands of T_2 symmetry may be expected at 28 517, 28 523 cm^{-1}.

Multiplets $^5L_9$, $^5G_3$ (Levels 50−64). These multiplets split into $A_1 + 4T_1 + E + 3T_2 + 2A_2$ states. The two photon bands overlap with those from $^5D_2$ and $^5G_4$, so that transition $N = 1$ to $N = 49$ ^5D_2E has been employed as a reference to present the relative TPA intensities.

For Cs_2NaTbF_6, the strongest peak for this multiplet is the $N = 1$ to $N = 51$ transition, with measured (calculated) relative intensity 1.5 (0.48) in (110a) for Cs_2NaTbF_6, and 1.2 (0.5) in (110a) for $Cs_2NaTbCl_6$. The $N = 1$ to $N = 62$ TPA transitions for both systems are predicted to be much weaker than measured. For Cs_2NaTbF_6, the intensities for the $N = 1$ to $N = 56$ $^5L_9$ E transition are measured (calculated) as 0.75 (0.64) in (100a) and 0.2 (0.16) in (110a). Other weak peaks observed in this region are calculated to be weaker.

Multiplets $^5L_{8,7,6}$, $^5G_2$ (Levels 65−85). For Cs_2NaTbF_6, the observed peaks are very weak, except the three at 29 337, 29 957, and 29 985 cm^{-1}, which were assigned to transitions from the ground state to terminal A_1 (65), E (78), and T_2 (77) levels. Taking the $N = 1$ to $N = 78$ transition as reference, then the measured (calculated) intensities are 0.3 (0.04) for $N = 1$ to $N = 65$, and 0.7, broad (2.5) in (110a) for $N = 1$ to $N = 77$. The relative intensities are not well predicted for $Cs_2NaTbCl_6$, and notably the transition $N = 1$ to $N = 65$ $^5L_8$ A_1 is predicted to be much weaker than observed.

Multiplets $^5D_{1,0}$, $^5H_7$ (Levels 86−93). All of the relative intensities in this region are well predicted, except that the intensity of the transition $N = 1$ to $N = 88$ $^5D_0A_1$ in Cs_2NaTbF_6 is underestimated.

Multiplets $^5H_{6,5,4}$ (Levels 94−107). These three multiplets are well-isolated from each other, in the range from 33 000 to 35 000 cm^{-1}. Taking the intensity of the $N = 1$ to $N = 99$ ^5H_6E transition as a reference, the relative TPE intensities in

Cs_2NaTbF_6 are well predicted, with deviation by no more than 3.7 times. The situation differs for $Cs_2NaTbCl_6$, where relative intensities for these three multiplets are poorly predicted. In may be relevant in this case that the experimental TPE spectra exhibit many unidentified peaks. It is also noted that the onset of $4f^7$5d configuration is ~34 000 cm^{-1} in $Cs_2NaTbCl_6$. The coupling of ungerade vibrations in $4f^7$5d states with $4f^8$ states may require consideration.

Remaining Multiplets: $^5F_{5,4,3}$, $^5I_{8,7}$, $^5H_3$, $^5G_6$, $^5K_6$ (Levels 108−174). TPE spectra were recorded up to 40 750 cm^{-1} for $Cs_2NaTbCl_6$ (i.e., up to level 174) but not for Cs_2NaTbF_6. The TPA intensities have been calculated for both systems in this energy range. Comparison with experimental results shows that the agreement between calculated and measured intensities is generally very poor for all multiplets in this region. Therefore descriptions of the comparison are neglected here.

CONCLUSIONS

First, the energy level calculations are considered. The major result has been the consistency of derived parameters, especially regarding CFPs, with those for other lanthanide ions in elpasolite hosts.[11] The original assignments[2] for Cs_2NaTbF_6 were used in our energy level parametrization to calculate CFPs and TPA intensities. Then the calculated TPA intensities and calculated energies were used to adjust the assignments. For Cs_2NaTbF_6, the differences in the energies of levels between the current and previous calculation[2] are mostly ca. 10 cm^{-1}, although in some cases, more than 20 cm^{-1}, for example, for $N = 67$ (24 cm^{-1}) and $N = 107$ (22 cm^{-1}). The revised assignments are very minor, as now detailed. First, the assignments for $^5D_2$,$^5L_9T_2$ ($N = 48, 51$) have been interchanged. The ^5L_9E level ($N = 56$) has been placed at 28 553 cm^{-1}. The parentage of the A_2 level at 29 037 cm^{-1} ($N = 61$) has been changed from $^5G_3$ to $^5L_9$. The parentages of $N = 65, 77, 78$ also differ from those in ref 2.

The crystal-field splittings of many multiplets of $Cs_2NaTbCl_6$ are smaller, and the overlapping of different multiplets is less, than for Cs_2NaTbF_6, so that experimental assignments of the crystal-field levels of Tb^{3+} in $Cs_2NaTbCl_6$ are more straightforward and definite. The differences in energies of CF levels of $Cs_2NaTbCl_6$ between the current and previous[3] calculations are generally less than 10 cm^{-1}. In Table 2, no changes have been made to the previously proposed energy level scheme for this system,[3] but the following reassignments may require further consideration. First, the TPA intensity calculations suggest the reassignment of the measured E-type level at 28 388 cm^{-1} to ^5G_4E ($N = 55$). Second, the measured level at 34 967 cm^{-1} may be reassigned to ^5I_8E, in view of the much stronger intensity of the transition from the ground state, despite the measured polarization independence. The *SLJ* parentages of some levels differ from those given in ref 3.

This study has presented the first detailed and definite comparison of measured TPE intensities for transitions between individual Stark levels, with intensities calculated by explicitly summing over all of the $4f^7$5d intermediate states, without neglecting $4f^7$ and 5d interactions. The wealth of experimental TPE intensity data presents a stringent test for calculations. The calculated TPA intensities are reasonably consistent with experimental results and do not call for revision of assignments, except in a few cases mentioned above.

Generally, the calculated TPA intensities exhibit better agreement with experiment for terminal multiplet terms of more pure Russell−Saunders parentage. Refinements to the present calculation may include the contributions from intermediate states such as from the $4f^7$5g configuration. Also, the TPE intensities of Tb^{3+} in the more ionic system Cs_2NaTbF_6 are well simulated by considering ED−ED contributions, but a more accurate prediction of TPA intensities for Tb^{3+} in $Cs_2NaTbCl_6$ needs to take other contributions into account. The inclusion of other intensity mechanisms, such as involving the participation of the ligand in dynamic coupling, appears to be essential.

AUTHOR INFORMATION

Corresponding Author

*E-mail: bhtan@cityu.edu.hk. Fax: 852 3442 0522. Phone: 852 3442 7840.

Notes

[§]E-mail: duanck@cqupt.edu.cn. Fax: 86 62471791. Phone: 86 15823864495.

ACKNOWLEDGMENT

Financial support for this work under the Chongqing Natural Science Foundation, Grant CSTC2010BB4403, and the Research Grants Council of Hong Kong, General Research Fund Grant CityU 102609, is gratefully acknowledged.

REFERENCES

(1) Berry, A. J.; Denning, R. G.; Morrison, I. D. *J. Chem. Phys.* **1997**, *106*, 8967.
(2) Berry, A. J.; Morrison, I. D.; Denning, R. G. *Mol. Phys.* **1998**, *93*, 1.
(3) Morrison, I. D.; Berry, A. J.; Denning, R. G. *Mol. Phys.* **1999**, *96*, 43.
(4) McCaw, C. S.; Denning, R. G. *Mol. Phys.* **2003**, *101*, 439.
(5) Berry, A. J.; McCaw, C. S.; Morrison, I. D.; Denning, R. G. *J. Lumin.* **1996**, *66&67*, 272.
(6) Berry, A. J.; Denning, R. G.; Morrison, I. D. *Chem. Phys. Lett.* **1997**, *266*, 195.
(7) Schwartz, R. W.; Brittain, H. G.; Riehl, J. P.; Yeakel, W.; Richardson, F. S. *Mol. Phys.* **1977**, *34*, 361.
(8) Faulkner, T. R.; Richardson, F. S. *Mol. Phys.* **1978**, *36*, 193.
(9) Thompson, L. C.; Serra, O. A.; Riehl, J. P.; Richardson, F. S.; Schwartz, R. W. *Chem. Phys.* **1977**, *26*, 393.
(10) Tanner, P. A.; Liu, Y. -L.; Chua, M.; Reid, M. F. *J. Alloys Compd.* **1994**, *207/208*, 83.
(11) Duan, C. -K.; Tanner, P. A. *J. Phys. Chem A* **2010**, *114*, 6055.
(12) Chen, X.; Liu, G.; Margerie, J.; Reid, M. F. *J. Lumin.* **2007**, *128*, 421.
(13) Zbiri, M.; Atanasov, M.; Daul, C.; Garcia-Lastra, J.-M.; Wesolowski, T. A. *Chem. Phys. Lett.* **2004**, *397*, 441.
(14) Zbiri, M.; Daul, C. A.; Wesolowski, T. A. *J. Chem. Theory Comput.* **2006**, *2*, 1106.
(15) Ruipérez, F.; Barandiarán, Z.; Seijo, L. *J. Chem. Phys.* **2005**, *123*, 244703.
(16) Ogasawara, K.; Watanabe, S.; Toyoshima, H.; Brik, M. G. *Handbook on the Physics and Chemistry of Rare Earths*; Gschneidner, K. A., Jr., Bünzli, J.-C., Pecharsky, V. K., Eds.; Elsevier Science B.V.: Amsterdam, 2007; Vol. 37, p 231.
(17) Reid, M. F.; Hu, L.; Frank, S.; Duan, C.-K.; Xia, S.; Yin, M. *Eur. J. Inorg. Chem.* **2010**, *18*, 2649.
(18) Görller-Walrand, C.; Binnemans, K. *Handbook on the Physics and Chemistry of Rare Earths*; Gschneidner, K. A., Jr., Bünzli, J.-C., Pecharsky, V. K., Eds.; Elsevier Science B.V.: Amsterdam, 1998; Vol. 25, p 101.

(19) Reid, M. F. *Crystal Field Handbook*; Newman, D. J., Ng, B., Eds.; Cambridge University Press: Cambridge, 2000; Ch. 10, p 193.
(20) Ceulemans, A.; Vandenburghe, G. M. *J. Chem. Phys.* **1993**, *98*, 9372.
(21) Ceulemans, A.; Vandenburghe, G. M. *J. Chem. Phys.* **1995**, *102*, 7762.
(22) Chua, M.; Tanner, P. A. *Acta Phys. Pol., A* **1996**, *90*, 169.
(23) Chua, M.; Tanner, P. A. *Phys. Rev. B* **1996**, *54*, R11014.
(24) Wang, D.; Ning, L.; Xia, S.; Tanner, P. A. *J. Phys.: Condens. Matter* **2003**, *15*, 2681.
(25) Burdick, G. W.; Burdick, A.; Deev, V.; Duan, C.-K.; Reid, M. F. *J. Lumin.* **2006**, *118*, 205.
(26) Duan, C.-K.; Tanner, P. A. *J. Phys.: Condens. Matt.* **2010**, *22*, 125503.
(27) Kundu, L.; Banerjee, A. K.; Chowdhury, M. *Chem. Phys. Lett.* **1991**, *181*, 569.
(28) Bouazaoui, M.; Jacquiert, B.; Linares, C.; Strek, W. *J. Phys.: Condens. Matt.* **1991**, *3*, 921.
(29) Reid, M. F.; van Pieterson, L.; Wegh, R. T.; Meijerink, A. *Phys. Rev. B* **2000**, *62*, 14744.
(30) van Pieterson, L.; Reid, M. F.; Wegh, R. T.; Soverna, S.; Meijerink, A. *Phys. Rev. B* **2002**, *65*, 045113.
(31) Tanner, P. A.; Duan, C.-K.; Makhov, V.; Kirm, M.; Khaidukov, N. M. *J. Phys.: Condens. Matt.* **2009**, *21*, 395504.
(32) Duan, C.-K.; Tanner, P. A.; Meijerink, A.; Babin, V. *J. Phys.: Condens. Matt.* **2009**, *21*, 395501.
(33) Judd, B. R.; Pooler, D. R. *J. Phys. C* **1982**, *15*, 591.
(34) Downer, M. C.; Cordero-Montalvo, C. D.; Crosswhite, H. *Phys. Rev. B* **1983**, *28*, 4931.
(35) Burdick, G. W.; Reid, M. F. *Phys. Rev. Lett.* **1993**, *70*, 2491.
(36) Burdick, G. W.; Reid, M. F. *Phys. Rev. Lett.* **1993**, *71*, 3892.
(37) Ning, L. X.; Wang, D. Y.; Xia, S. D.; Thorne, J. R. G.; Tanner, P. A. *J. Phys.: Condens. Matt.* **2002**, *14*, 3833.
(38) Reid, M. F.; Richardson, F. S. *Phys. Rev. B* **1984**, *29*, 2830.